Available online at www.sciencedirect.com
SCIENCE DIRECT®
Journal of Solid State Chemistry 175 (2003) 218–225
JOURNAL OF SOLID STATE CHEMISTRY
http://elsevier.com/locate/jssc

A new type of charge compensating mechanism in $Ca_5(PO_4)_3F:Eu^{3+}$ phosphor

R. Sahoo, S.K. Bhattacharya, and R. Debnath*

Central Glass and Ceramic Research Institute, 196, Raja S.C. Mullick Road, Kolkata 700 032, India

Received 4 December 2002; received in revised form 21 April 2003; accepted 5 May 2003

Abstract

The X-ray powder diffraction, reflectance, photoluminescence, photoluminescence excitation and ESR spectra of $Ca_5(PO_4)_3F:Eu^{3+}$ phosphor have been studied. Three distinct variants of calcium substitutional Eu^{3+}-sites have been observed in this host and the charge compensating species related to each of these sites has been identified. It is noted that the host related trace impurities those have prospects of acting as charge compensator, and the reaction environment that exists during the preparation of the material, greatly influence the preferential substitution of different Ca^{2+}-sites by the Eu^{3+} ions. It is also noted that the charge compensating species in a suitable case, takes part in the photophysical process of luminescence of the Eu^{3+}.

Keywords: Eu^{3+} in fluoroapatite; Charge balance; Photoluminescence; CT-states; Dipolar complex

1. Introduction

Alkaline earth haloapatites, $M_5^{II}(PO_4)_3X$ (M = Mg, Ca, Sr, Ba and X = F, Cl, Br) are used as host for the preparation of transition metal/rare earth ion based various commercial lamp phosphors [1,2]. Rare earth ions in such a host experience a large splitting of their energy levels as well as high emission cross-section because of relatively high induced crystal field effect and for this reason; several rare earth activated haloapatites, fluoroapatite in particular, have been explored [3–6] for their possible use also as solid state laser medium.

The crystal structure of fluoroapatite [$Ca_5(PO_4)_3F$], was first studied by Naray Szabo [7] and subsequently it has been investigated by many others [8–10]. It belongs to the hexagonal space group $p6_3/m$ with unit cell formula $Ca_{10}(PO_4)_6F_2$, and $a = b = 9.36$ Å, $c = 6.88$ Å. A unit cell consists of four layers with dispositions [8] of its ions as illustrated in Fig. 6. Each of the Ca^{2+} ions lying in the plane $Z = 0$ and $2C/4$ has three-fold symmetry C_3 axis parallel to the Z-axis and is nine-fold coordinated by oxygen ions. Six oxygen ions are near neighbor to Ca^{2+} and the other three oxygen ions are somewhat further away. This cationic site is known as site-I. The Ca^{2+} ions in the $Z = C/4$ and $3C/4$ planes do not have any symmetry axis, but are located in the symmetry plane of the crystal. Each of the Ca^{2+} ion of this site which had been designated as site-II, is seven-fold coordinated with C_s point group symmetry. Six oxygen ions and a fluoride ion are the ligands. The fluoride ion is located in the same plane as near neighbor of Ca^{2+} at a distance 2.35 Å.

Preferential occupancy of substitutional Ca^{2+}-sites by a trivalent large cation in apatite has been studied by a number of workers [8,11,12]. Blasse [11] first proposed that the principle of local charge compensation, could predict the site occupancy by a trivalent ion in an apatite. For a trivalent ion in site-II, the original C_s symmetry may be retained only when the site symmetry is not lowered by the presence of the charge compensating species. In fact, the point group C_s is retained if the compensating species resides [4] in the symmetry plane of the group. And possibly for this reason, when a trivalent ion is incorporated in this host, the ion normally enters into site-II, facilitating [4,8,14] the process of charge balance through substitution of the fluoride ion (F^-) on the symmetry plane by an oxygen ion (O^{2-}).

Spectroscopic properties of Eu(III) ions in fluoroapatite, have been studied in the past [13–17]. Voronko et al. [14] studied the polarized photoluminescence properties

*Corresponding author. Fax: +91033-2473-0957.
E-mail address: debnath@cgcri.res.in (R. Debnath).

0022-4596/$ - see front matter © 2003 Elsevier Inc. All rights reserved.
doi:10.1016/S0022-4596(03)00249-4

of Eu(III) in fluoroapatite single crystal and suggested that Eu(III) ion in this host reside in the Ca^{2+}-II site with C_s symmetry. Jagannathan and his group [15] from their photoluminescence study also concluded that Eu(III) ions in this host mainly occupy Ca^{2+}-II sites, but due to the influence of charge compensating species the local symmetry gets transformed from C_s to tetragonal. Gaft et al. [16] made comparative study of the spectroscopic property of Eu(III) in natural apatite vis-à-vis that of the ion in synthetic apatite and found that Eu(III) ions in natural apatite mainly occupy the Ca^{2+}-I sites and charge compensation in the system is achieved with the introduction of an impurity Na(I) ion in the neighboring calcium substitutional site ($2Ca^{2+} = Eu^{3+} + Na^{+}$). Recently Karbowiak et al. [17] reported that the nature of site occupancy by Eu(III) ions in calcium fluoroapatite varied with the variation of the method of preparation of the material.

Thus, understanding of the mechanism of preferential site occupancy by trivalent lanthanide ions in fluoroapatite, and the role charge compensator in this process is far from complete. In the present work, we have revisited the system.

2. Experimental

2.1. Materials preparation

The phosphor $Ca_5(PO_4)_3F:Eu^{3+}$, was prepared by using a homogeneous mixture of composition (mole %): $CaCO_3 = 53.5$, $CaF_2 = 23$, $P_2O_5 = 23$, and $Eu_2O_3 = 0.5$. Phosphoric acid was taken as the source of P_2O_5. Europium oxide used, was of 99.9% pure grade (Aldrich). All other chemicals were of GR grade (E Merck). The reaction mixture was taken in a platinum crucible and slowly heated in an electrical furnace at a rate of 8°C/min to reach up to 600°C. It was allowed to stay at that temperature for 1 h to facilitate evolution of CO_2 and H_2O. Then the temperature was raised to 900°C at a rate of 8°C/min, and finally to 1200°C at a rate of 6°C/min. Reaction at final temperature was allowed to continue for 15 min. The product was a white sintered cake. It was cooled and then crushed to polycrystalline powder.

2.2. Measurements

To check the purity of the phase, X-ray powder diffraction spectrum of the material was recorded at 300 K in a Philips Analytical X-ray diffractometer (PW1710) with a copper anode (wavelengths: $\alpha_1 = 1.54056$ Å, $\alpha_2 = 1.54439$ Å). The experimental scanning parameters were: step size [°2θ] = 0.040°, step time = 0.250 s and smooth factor = 2.

Reflectance spectra of the phosphor were measured at 300 K in an UV-VIS-NIR absorption Spectrometer (Shimadzu UV-VIS-NIR 3101 PC, Japan) equipped with reflectance measurement accessories. The excitation dependent photoluminescence spectra and lamp-corrected excitation spectra corresponding to different photoluminescence were measured at 300 K, in a Perkin Elmer Spectrofluorimeter (Model: LS-55, UK). Electron spin resonance (ESR) spectra were also recorded at 300 K in a JEOL-JES X-band ESR spectrometer (Model: JEOL-JES RE 1X, Japan) with a frequency modulation ±100 kHz.

3. Experimental results

3.1. X-ray powder diffraction spectrum

The X-ray powder diffraction spectrum of the Eu^{3+} activated fluoroapatite studied is shown in Fig. 1. Twenty lines of significant intensity of the spectrum were fitted to determine their indices and the crystallographic parameters of the phase, using the program DICVOL 91. The results obtained are in fact, a reproduced version of those reported [9] in the standard data file for calcium fluoroapatite. These are tabulated in Table 1, which show that the phase grown, belongs to a hexagonal system of space group $p6_3/m$ with $a_0 = 9.36$ Å, $c_0 = 6.88$ Å.

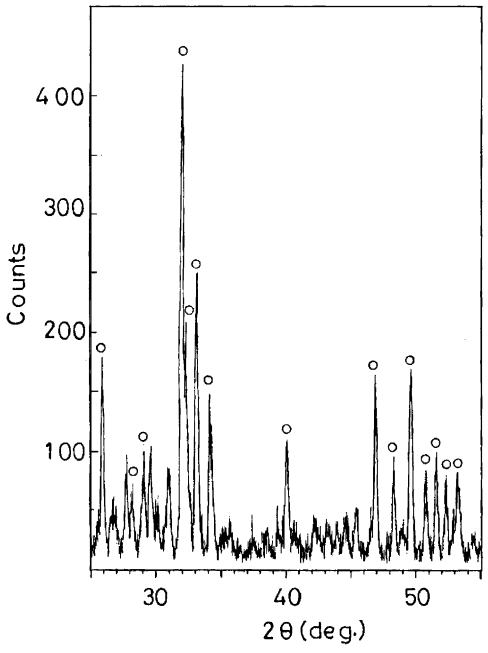

Fig. 1. X-ray powder diffraction spectrum of the $Ca_5(PO_4)_3F:Eu^{3+}$ at 300 K. ○ points to the lines of the apatite phase.

3.2. Reflectance spectra

The reflectance spectra of the phosphor is shown in Figs. 2a and b. It shows a broad absorption band around 245–250 nm and a change in slope in between 270–280 nm in the UV region (Fig. 2a). In the VIS-region (Fig. 2b), the expected series of absorption lines of Eu(III) are also discernible.

A comparison of the energies of the bands with those of the absorption bands of Eu^{3+} in different hosts reported in the literature [18–20,23], allowed us to assign tentatively, the absorption bands of Eu^{3+} in this phase as follows: 361 nm ($^7F_0 \rightarrow {}^5D_4$), 395 nm ($^7F_0 \rightarrow {}^5L_6$), and 464 nm ($^7F_0 \rightarrow {}^5D_2$). The excitation spectra recorded for different luminescence of Eu(III) in this host also support the above assignment. A more resolved version of the spectrum, however, shows (Fig. 2b, inset) an additional absorption shoulder around 398 nm overlapping with the 395 nm ($^7F_0 \rightarrow {}^5L_6$) band. This new shoulder at 398 nm does not seem to be the $^7F_0 \rightarrow {}^5D_3$ transition of Eu^{3+} because; (a) ΔJ in this case is 3, so the $^7F_0 \rightarrow {}^5D_3$ transition is a forbidden transition. (b) The energy of this transition, lies [18] around 24,490 cm^{-1} (408 nm), which is much lower than that of the 398 nm band (25,125 cm^{-1}).

Table 1

d (A)	Int.	h	k	l
8.14	8	1	0	0
5.26	4	1	0	1
4.05	8	2	0	0
3.867	8	1	1	1
3.438	40	0	0	2
3.16	14	1	0	2
3.067	18	2	1	0
2.804	100	2	1	1
2.77	55	1	1	2
2.703	60	3	0	0
2.624	30	2	0	2
2.288	8	2	1	2
2.252	20	3	1	0
1.937	25	2	2	2
1.884	14	3	1	2
1.838	30	2	1	3
1.796	16	3	2	1
1.771	14	4	1	0
1.746	14	4	0	2
1.721	16	0	0	4

3.3. Photoluminescence spectra

In the crystal field with C_3 symmetry the multiplets $^7F_0$, $^7F_1$, and $^7F_2$ of Eu(III) are expected to split into one, two and three components respectively, where as in the field of C_s symmetry, the orbital degeneracy is completely lifted and one, three and five components of the appropriate multiplets appear.

The Photoluminescence spectrum of the phosphor under 251 nm-excitation, is shown in Fig. 3a. It shows weak emission around 579 nm due to forbidden $^5D_0 \rightarrow {}^7F_0$ transition but strong emission at 588 and 594 nm due to $^5D_0 \rightarrow {}^7F_1$ magnetic dipole-allowed transition and at 613, 618 and 623 nm due to hypersensitive $^5D_0 \rightarrow {}^7F_2$ transition. Weak emission bands at 652 and 698 mm, respectively, due to $^5D_0 \rightarrow {}^7F_3$ and $^5D_0 \rightarrow {}^7F_4$ transitions are also observed.

The photoluminescence spectrum obtained upon 325 nm-excitation (Fig. 3b) however, drastically differ from the one described above. The $^5D_0 \rightarrow {}^7F_0$ transition in this case, becomes most intense and appears around 572 nm. A number of components of the band due to $^5D_0 \rightarrow {}^7F_1$ and $^5D_0 \rightarrow {}^7F_2$ transitions overlapping with one another in the spectral range 582–630 nm are observed. Taking into consideration the experimental results of Voronko et al. on the stark components of $^7F_{j=1,2}$ multiplets of Eu^{3+} in apatite single crystal,

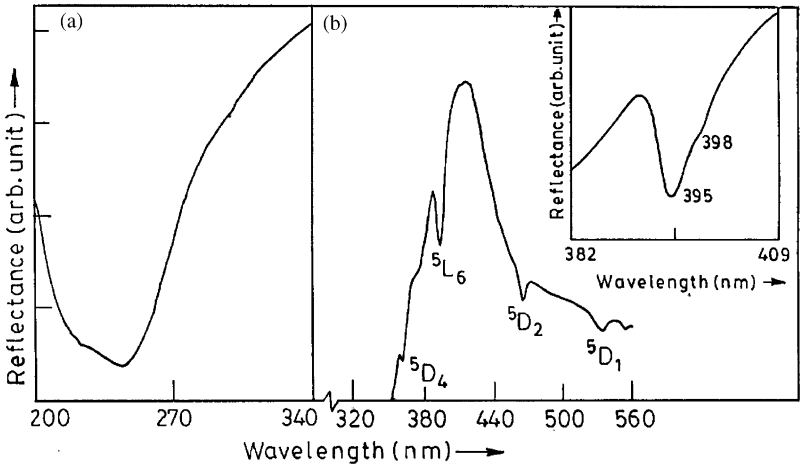

Fig. 2. Reflectance spectrum (a, b) of the $Ca_5(PO_4)_3F:Eu^{3+}$ at 300 K. Inset: a highly resolved version of a part of the spectrum (b).

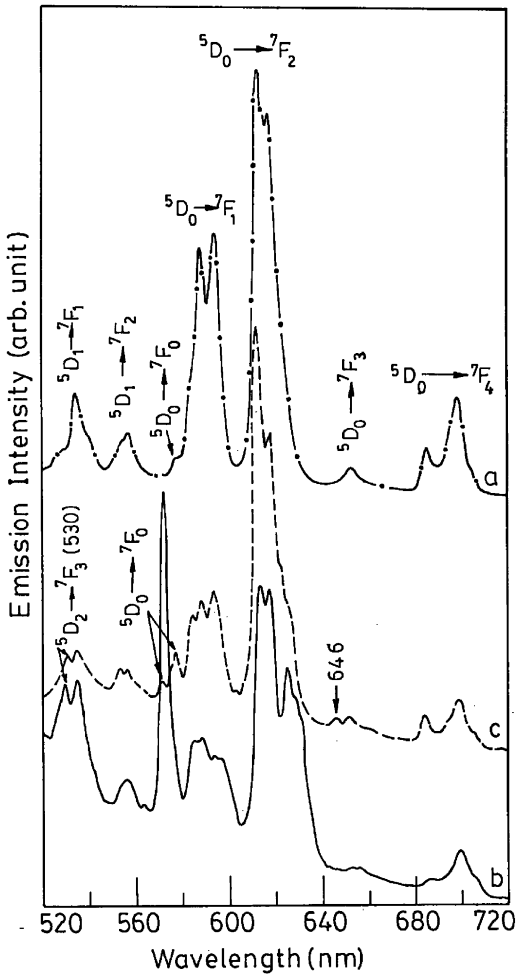

Fig. 3. Emission spectra of the $Ca_5(PO_4)_3F:Eu^{3+}$ at 300K under different excitation: (a) $\lambda_{Excitation} = 251$ nm, (b) $\lambda_{Excitation} = 325$ nm and (c) $\lambda_{Excitation} = 276$ nm.

components of the $^5D_0 \rightarrow {}^7F_1$ transition of the present system can be identified as 582 and 613 nm while those of $^5D_0 \rightarrow {}^7F_2$ transition as 597, 625 and 628 and 630 nm.

Upon excitation with 276 nm radiation, the same material exhibits a third type of its photoluminescence (Fig. 3c). The $^5D_0 \rightarrow {}^7F_0$ luminescence band in this case, occurs at 577 nm with some what lower intensity. The stark components of the luminescence bands due to $^5D_0 \rightarrow {}^7F_1$ and $^5D_0 \rightarrow {}^7F_2$ transitions, in this case also, appear over lapping with one another and can be distinguished in the light of Voronko's results as follows: the components of $^5D_0 \rightarrow {}^7F_1$ transition are 584, 612 nm bands; the similar components of the hypersensitive $^5D_0 \rightarrow {}^7F_2$ transition are 594 nm band and three weak shoulders at around 622, 625 and 632 nm. The luminescence band due to $^5D_0 \rightarrow {}^7F_3$ transition distinctly appears here, at 646 nm.

Consideration of the splitting pattern of the bands of $^5D_0 \rightarrow {}^7F_1$ (two components) and $^5D_0 \rightarrow {}^7F_2$ (three components) transitions of the spectrum obtained upon excitation with 251 nm radiation suggests that the Eu(III) centers related to this luminescence have site-symmetry C_3, i.e., the Eu(III) ions associated with this luminescence reside in Ca^{2+}-I substitutional sites.

The relative high energy of $^5D_0 \rightarrow {}^7F_0$ transitions as well as greater number of split components of the $^7F_1$ and $^7F_2$ multiplets in each of the emission spectrum obtained on excitation, respectively, with the 276 and 325 nm radiation, suggest that Eu(III) centers related to these two cases of luminescence reside at the Ca^{2+}-II location of the host.

Interestingly, in this host, luminescence emission of weak intensity from upper $^5D_1$ level are also observed at 535 and 556 nm, respectively, due to $^5D_1 \rightarrow {}^7F_1$ and $^5D_1 \rightarrow {}^7F_2$ transitions, for each case of the above mentioned three excitations (namely, 251, 276 and 325 nm). An additional luminescence band at 529 nm is however, also observed in the cases of 276 and 325 nm excitations but not in the case of 251 nm excitation. Consideration of energy and sharpness of the 529 nm band indicate that it is most likely related to $^5D_2 \rightarrow {}^7F_3$ transition of Eu^{3+}. Rationale for such assignment is further given in the discussions.

3.4. Photoluminescence excitation spectra

Lamp corrected excitation spectrum of the three different $^5D_0 \rightarrow {}^7F_0$ emissions as well as that of 529 nm emission are shown, respectively in Figs. 4a–d. The excitation spectrum of 579 nm ($^5D_0 \rightarrow {}^7F_0$) luminescence (Fig. 4a), shows a band at 251 nm along with all the absorption bands of Eu(III). The energy of the 251 nm band is comparable to that of the CT-band reported by Gaft et al. [16] for Eu^{3+} in Ca^{2+}-I site we therefore, assign the observed 251 nm band as the CT band of Eu^{3+} in Ca^{2+}-I site.

Excitation spectrum of 572 nm ($^5D_0 \rightarrow {}^7F_0$)-luminescence (Fig. 4c), shows a similar feature excepting that in this case, the CT band [16] is split into two bands occurring at 280 and 325 nm. The same of 577 nm ($^5D_0 \rightarrow {}^7F_0$)-luminescence transition (Fig. 4b), also exhibits CT band which is triply split with components at 254, 276 and 320 nm.

The excitation spectrum of the 529 nm emission (Fig. 4d), however, also shows the split CT band with components at 254, 276 and 330 nm but does not show all the absorption feature of Eu(III). Instead, it exhibits only one sharp band at 397 nm (similar to the one detected earlier, in the highly resolved reflectance spectra of the phosphor around 398 nm).

The 397 nm band can not be assigned to $^7F_0 \rightarrow {}^5L_6$ of Eu(III) of a new site, because in that case, the observed phenomenon of noninvolvement of other absorption bands of Eu(III) in the process of 529 nm emission can not be rationalized.

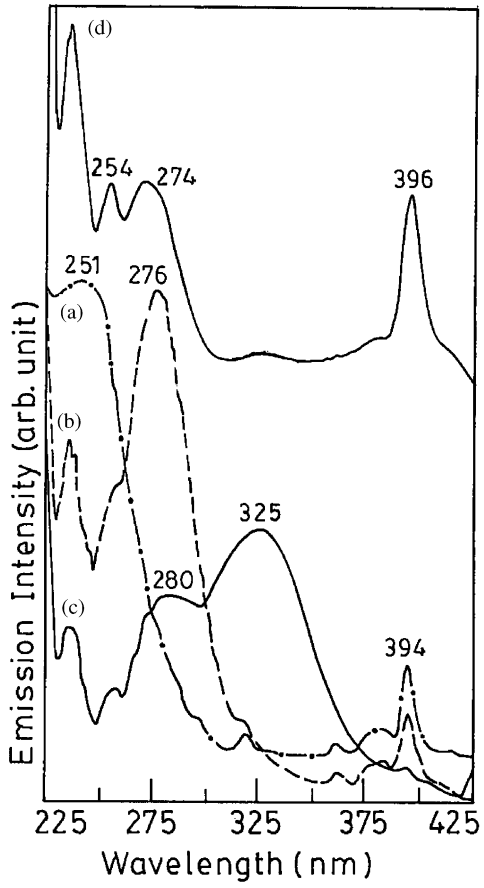

Fig. 4. Excitation spectra of the $Ca_5(PO_4)_3F:Eu^{3+}$ at 300 K for different luminescence emissions: (a) $\lambda_{Monitored} = 579$ nm, (b) $\lambda_{Monitored} = 577$ nm, (c) $\lambda_{Monitored} = 572$ nm and (d) $\lambda_{Monitored} = 529$ nm.

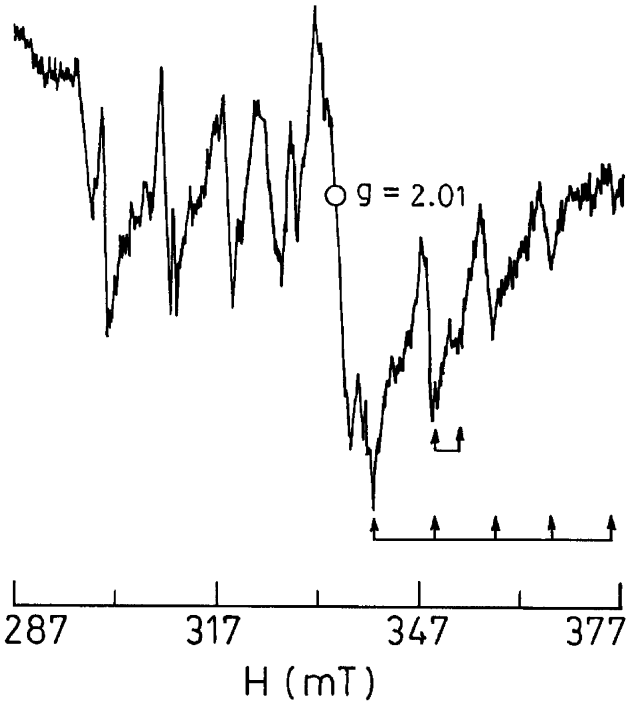

Fig. 5. ESR spectrum of the $Ca_5(PO_4)_3F:Eu^{3+}$ at 300 K.

3.5. ESR spectrum

ESR spectrum of the phosphor is shown in Fig. 5. While the host itself, does not give any ESR signal, the phosphor exhibits a weak ESR signal of mean 'g' ~ 2.01 which consists of a series of weak lines of separation of ~ 9 mT. In some cases, these lines are further weakly split with a separation of ~ 2.5–3.0 mT. The values of $g = 2.01$ and hyperfine splitting of ~ 9.0 mT indicate [24,25] that the related paramagnetic species is most likely a polynuclear fluoride hole center $(F_{2n})^-$ type.

Considering the fact that a significant amount of calcium fluoride was used as one of the ingredients for the preparation of the present phosphor, the reaction environment during the preparation of the material, must had plenty of free fluorine. Under such a condition, trapping of molecular fluorine in the interstitial of the host is quite possible.

In case of a hole center of multinuclear fluorine cluster a number of hyperfine lines with a relatively smaller separation are expected [24,25] in its ESR spectrum because of mutually interacted hyperfine effect of the different fluorine nuclei ($I = 1/2$). Further splitting of the lines with a separation of 2.5–3.0 mT seems to be due to the hyperfine effect of Eu-nucleus ($I = 5/2$). The results suggest that the paramagnetic fluoride cluster is located near the Eu(III) ions and are involved in a bonding process with the former.

It is logical therefore to assume that $(F_{2n})^-$ type holes detected in the ESR spectrum are the charge-compensating species for some of the Eu(III) ions in this host.

There are a number of reports [26–28] in literature of identifying and characterizing such alkaline earth metal ion (M = Ca, Sr, Ba) substituted lanthanide ion plus interstitial trapped F^- dipolar complex pair in various cases of lanthanide ions doped MF_2 fluoride crystals. Baker et al. [27] studied in detail about the structure of such defects from ENDOR measurements.

The intensity of the ESR signal of the $(F_{2n})^-$ holes is weak which indicates that the population of such hole center in the host is low. The result suggests that only a fraction of Eu^{3+} ions present in the system has $(F_{2n})^-$ as the charge compensator. It is known from literatures [24,25] that the halide ions in the network structure of a solid help trapping multinuclear halogen cluster in the host. In case of fluoroapatite structure, fluoride ions are present only with the Ca^{2+}-II site, so the $(F_{2n})^-$ holes can permanently exist only at this site to act as charge compensator. However, since the material was prepared in the open, the charge compensation of Eu(III) of this site by atmospheric oxygen through replacement of fluoride ions is also equally possible.

4. Discussions

The totally forbidden non-degenerate $^5D_0 \rightarrow {}^7F_0$ transition which becomes allowed [18,22] only for sites of C_{nv} or lower symmetry, due to the presence of a linear term in the Hamiltonian of the respective crystal field [21], and gains strength from mixing of positive 'j' values in one or both the levels, is generally used [21,22] to identify the number of lanthanide sites present in a host. The three $^5D_0 \rightarrow {}^7F_0$ emissions observed at 572, 577 and 579 nm upon three different excitations thus clearly indicate that they represent three different sites of Eu(III) ions in this host.

In Ca^{2+}-I site the $Ca^{2+}\cdots O^{2-}$ distance is relatively large [10,16]. If one considers that this distance is retained even when the Ca^{2+} ion is substituted by Eu^{3+} ion, the energy of the $Eu^{3+}\cdots O^{2-}$ CT-state should be high. The observed 251 nm CT-state is therefore, seems to be related to Eu^{3+} ions in Ca^{2+}-I sites. The assignment is quite in agreement with the observed splitting feature of the $^7F_1$ (2 components) and $^7F_2$ (3 components) multiplets in the related luminescence spectrum. In this site, an Eu(III) ion is surrounded by nine oxygen atoms and the charge compensation is known to be accomplished [16] by the entry of an impurity Na^{+1} ion in a neighboring Ca^{2+} position. The related charge balance equation may be written as $2Ca^{2+} = Eu^{3+} + Na^{+1}$. Since the newly accommodated Na^{+1} ion is located much away from the Eu^{3+}-site, the symmetry of the oxygen coordination structure is not expected to be very much disturbed and so no splitting of the CT state (251 nm) is observed. We designate this Eu^{3+}-center as Eu^{3+}–Ca^{2+} I(Na^+).

The distance between $Ca^{2+}\cdots O^{2-}$ of the Ca^{2+}-II site, on the other hand is relatively shorter [7,10] (2.39 Å). So for Eu^{3+} ions in Ca^{2+}-II sites, $Eu^{3+}\cdots O^{2-}$ distance should also be relatively short and hence energy of the CT state is expected to be lower compared to that of the CT-state for Eu^{3+} ion in Ca^{2+}-I site. A Eu^{3+} ion in Ca^{2+}-II site, is coordinated by six oxygens and one fluoride ion. Charge compensation for introduction of a trivalent ion in this site, is generally known [4,8] to occur by replacement of the fluoride ion of coordination structure by an oxide ion. This seventh oxide ion being free (i.e., not associated with phosphorous), it comes closer to the Eu^{3+} ion to form covalent bond [12]. The distance between the Eu^{3+} ion and the seventh oxygen thus, attains a minimum value of 2.35 Å (sum of their ionic radii). The asymmetry in the distance of this seventh oxygen from the others, possibly causes a distortion in the C_s symmetry of the site and as a consequence induces a splitting in its CT-state. In this lower symmetry crystal field one should observe a relatively larger intensity of the $^5D_0 \rightarrow {}^7F_0$ transition due to J-mixing and the $^5D_0$ level should be shifted towards higher energy.

The excitation spectrum of 572 nm-emission showed a CT band split at 280 and 325 nm. The number of split components of the $^7F_1$, and $^7F_2$ multiplets in the related emission spectrum indicated C_s symmetry for this site. It is therefore rational to associate this Eu^{3+}-site to (Ca^{2+} II) location. The related charge compensation mechanism in this case, is $Ca^{2+} + F^{1-} = Eu^{3+} + O^{2-}$. We write this Eu^{3+} center as Eu^{3+}–Ca^{2+} II(O).

Since the CT state of the 577 nm emission is found to be split into three components (254, 276 and 320 nm), it seems that Eu^{3+} ions of 577 nm emission, although reside in the Ca^{2+}-II site, is some what different from that of Eu^{3+} in Ca^{2+} II(O) site.

It is evident from the EPR results that for a fraction of Eu(III) in Ca^{2+}-II sites, the associated charge compensating species is $(F_{2n})^-$ hole which grows by the influence of the fluoride ion of the coordination sphere as shown schematically in Fig. 6. Since in this case, the charge compensating species, i.e., $(F_{2n})^-$ hole lies in the symmetry plane of the of the group, the original C_s symmetry of the site is retained.

Again under such an arrangement a possibility of formation of a dipolar complex of the $[Eu^{3+}\cdots(F_{2n})^-]$ type, in the ground state due to partial de-localization of unpaired electron of the fluoride holes towards the Eu(III) ion also arises. The 397/398 nm new absorption

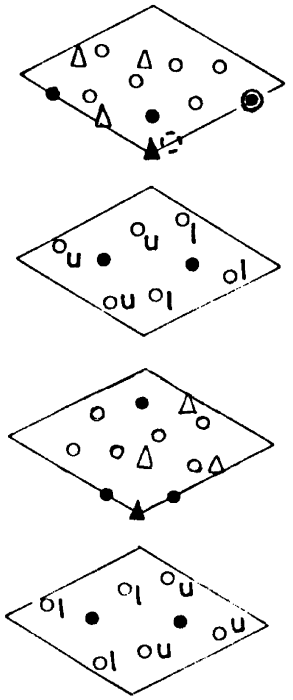

Fig. 6. Atomic layers in the crystal lattice of fluoroapatite. Lattice constants $c = 9.36$, $a = 6.88$ Å. The C_6 axis is perpendicular to the plane of the drawing. ● = Calcium, O = Oxygen, △ = phosphorous, ▲ = Fluoride ion, ◌ = possible position of $(F_{2n})^-$ ion and ◉ = possible position of Eu^{3+} ion. The suffice u and l on oxygen ions of the figure denote that the relevant oxygen ions are located at $C/16$ above or below the plane, respectively.

band that occurs in the excitation as well as the reflectance spectra of the phosphor seems to be associated with this complex.

The large size of the $(F_{2n})^-$ hole and its formation of dipolar complex with Eu^{3+} should have a perturbing effect on Eu(III) of this site. This effect possibly, induces a splitting of the associated charge transfer state into a triplet (254, 276 and 320 nm). The charge balance equation of this site may be written as $Ca^{2+} = Eu^{3+} + (F_{2n})^-$ and the center may be expressed as Eu^{3+}–Ca^{2+} II$(F_{2n})^-$. The three Eu^{3+}-centers identified, and their spectroscopic properties have been summarized in Table 2.

The higher excited state of Eu^{3+} ions in an oxide or phosphate host is normally found to deactivate by cascading directly down to the lowest $^5D_0$ excited state and the emission of Eu^{3+} ions in such a host is observed only from $^5D_0$ level. In case of Eu^{3+}–Ca^{2+}-II $(F_{2n})^-$ site, the 397 nm level of the dipolar complex lies in between the CT state (330 nm) and lowest $^5D_0$ level (589 nm) of Eu^{3+} and hence it may get involved in the deactivation process when the Eu^{3+} ions of this center are excited. Thus an excited Eu^{3+} ion of this center may reach to its $^5D_2$ and $^5D_1$ states via the excited state energy level of the complex.

Because of the fact that the dipolar $[Eu^{3+}\cdots(F_{2n})^-]$ complex in the excited state may attain a structure where the unpaired electron of the fluorine cluster, shifts to the europium ion and the europium ion on receiving the electron reaches to a metastable state $(Eu^{3+})^-$, relaxation of higher excited state of Eu^{3+} via the dipolar complex may exhibit following phenomena: (1) a major rearrangement of the $^5D_2$ state of Eu^{3+} with respect to its $^7F_3$ state and (2) a greater coupling of the states with the weak phonons of the fluoride cluster anion. This phenomenon possibly helps observation of 529 nm emission due to the $^5D \rightarrow {}^7F_3$ transition and brings about a significant lowering of its energy (e.g. from 19,600 to 18,900 cm^{-1}).

Another important point to note in this context is that the phosphor gives 529 nm-emission even when the Eu^{3+} ions of Ca^{2+}-II (O) site are excited with 325 nm radiation. This is possibly because, the lowest energy component of the CT band of Eu^{3+}–Ca^{2+}II $(F_{2n})^-$ center lies around 320 nm, i.e., just above the 325 nm CT state of Eu^{3+}–Ca^{2+}II (O) center, so energy transfer from the Eu^{3+}–Ca^{2+}II (O) center to the Eu^{3+}–Ca^{2+}-II $(F_{2n})^-$ center is quite possible when the former is excited with 325 nm.

Table 2
Different Eu^{3+} centers in the apatite studied

Center	CT bands (λ nm)	Reported data on stark splitting [14]	Emission (λ nm)	Transition	Charge balance
Eu^{3+}–Ca^{2+} I(Na^+)	251	—	579	$^5D_0 \rightarrow {}^7F_0$	$2Ca^{2+} = Eu^{3+} + Na^{1+}$
		—	588	$^5D_0 \rightarrow {}^7F_1$	
		—	594		
		—	613	$^5D_0 \rightarrow {}^7F_2$	
		—	618		
		—	623		
Eu^{3+}–Ca^{2+}II (O)	280, 325	572	572	$^5D_0 \rightarrow {}^7F_0$	$Ca^{2+} + F^{1-} = Eu^{3+} + O^{-2}$
		577	—	$^5D_0 \rightarrow {}^7F_1$	
		582	582		
		612	613		
		597	597	$^5D_0 \rightarrow {}^7F_2$	
		599	—		
		624	625		
		628	628		
		630	630		
Eu^{3+}–Ca^{2+}II $(F_{2n})^-$	254, 276, 320		577	$^5D_0 \rightarrow {}^7F_0$	$Ca^{2+} = Eu^{3+} + (F_{2n})^-$
			—	$^5D_0 \rightarrow {}^7F_1$	
			584		
			612		
			594	$^5D_0 \rightarrow {}^7F_2$	
			—		
			622		
			625		
			632		
			529	$^5D_2 \rightarrow {}^7F_3$	

Acknowledgments

The authors thank Dr. Sukhen Das, CGCRI, Kolkata, for recording the X-ray diffraction spectrum and the Director of CGCRI, Kolkata, India, for his encouragement. The present work has been carried out under the sponsorship (No. SP/S2/M-65/96) of Department of Science and Technology, Government of India.

References

[1] J.L. Ouweltjes, Philips Tech. Rev. 13 (1951) 346.
[2] S. Shionoya, W.M. Yen (Eds.), Phosphor Handbook, CRC Press LLC, Boca Raton, FL, 1999.
[3] M.J. Weber, in: H.M. Crosswhite, H.W. Moos (Eds.), Optical Properties of Ions in Crystals, Wiley-Interscience, New York, 1967.
[4] A.A. Kaplyanskii, E.G. Kuzminov, Opt. Spectrosc. 29 (1970) 376.
[5] F.M. Ryan, R.W. Warren, R.H. Hopkins, J. Murphy, J. Electrochem. Soc. 125 (1978) 1493.
[6] S.A. Payne, L.D. Deloach, L.K. Smith, W.L. Kway, J.B. Tassano, W.F. Krupke, H.T. Chai, G. Loutts, J. Appl. Phys. 76 (1994) 497.
[7] S. Naray-Szabo, Z. Kristallogr. 75 (1930) 387.
[8] K. Narita, J. Phys. Soc. (Japan) 16 (1961) 99.
[9] (a) Standard X-ray diffraction powder pattern, NBS Monograph, Vol. 25 (3), 1964, p. 22;
(b) JCPDS Card No. 15-0876 (1972).
[10] M. Slansky, Geol. Phosphates Sedimentaries Mem., BRGM (1980).
[11] G. Blasse, J. Solid State Chem. 14 (1975) 181.
[12] B. Piriou, D. Fahmi, J. Dexpert-Ghys, A. Taitai, L.J. Lacout, J. Lumin. 39 (1987) 97.
[13] B.S. Gorobets, Opt. Spectrosc. 25 (1968) 154.
[14] Y.K. Voronko, G.V. Maksimova, A.A. Sobol, Opt. Spectrosc. 70 (1991) 346.
[15] R. Jagannathan, M. Kottaisamy, J. Phys.: Conden. Matter 7 (1995) 8453.
[16] M. Gaft, R. Reisfeld, C. Panczer, S. Shoval, B. Champagnon, G. Boulon, J. Lumin 72–74 (1997) 572.
[17] M. Karbowiak, S. Hubert, J. Alloys Compds. 302 (2000) 87.
[18] B. Blanzat, L. Boehm, C.K. Jorgensen, R. Reisfeld, N. Spector, J. Solid State Chem. 32 (1980) 185.
[19] R. Reisfeld, E. Greenberg, R.N. Brown, M.G. Drexhage, C.K. Jorgensen, Chem. Phys. Lett. 95 (1983) 91.
[20] M. Dejneka, E. Snitzer, R.E. Riman, J. Lumin. 65 (1995) 227.
[21] J. Holsa, M. Leskela, Mol. Phys. 54 (1985) 657.
[22] W. Xu, W. Jia, I. Revira, K. Monge, H. Liu, J. Electrochem. Soc. 148 (2001) H176.
[23] R. Sahoo, S.K. Bhattacharya, R. Debnath, J. Mater. Res 18 (2003) 609.
[24] D.L. Griscom, J. Non-Cryst. Solids 161 (1993) 45.
[25] L.D. Bogomolova, Yu.G. Teplyakov, V.A. Jachkin, V.L. Bogdanov, V.D. Khalilev, F. Caccavale, S. LoRusso, J. Non-Cryst. Solid 202 (1996) 178.
[26] S.H. Ong, P.W.M. Jacobs, J. Solid State Chem 32 (1980) 193.
[27] J.M. Baker, E.R. Davies, J.P. Hurrell, Proc. Roy. Soc. London Ser. A 308 (1968) 403.
[28] A.D. Franklin, J.M. Crissman, K.F. Young, J. Phys. C: Solid State Phys. 8 (1975) 1244.